

Finite-Time Attitude Control of Uncertain Quadrotor Aircraft via Continuous Terminal Sliding-Mode-Based Active Anti-Disturbance Approach

Omar Mechali^{1,2,*}, Jamshed Iqbal³, Abdesselam Mechali⁴, Xiaomei Xie^{1,2}, Limei Xu^{1,2}

¹School of Aeronautics and Astronautics, University of Electronic Science and Technology of China, Chengdu, 611731, China

²Aircraft Swarm Intelligent Sensing and Cooperative Control Key Laboratory of Sichuan Province, UESTC, China

³Department of Computer Science and Technology, Faculty of Science and Engineering, University of Hull, HU6 7RX, UK

⁴Department of Mechanical Engineering, University of Hassiba Ben Bouali, Chlef, Algeria

*Corresponding author: mechali.omar@std.uestc.edu.cn

Abstract - This research addresses the problem of robust attitude control for a quadrotor operating in an environment polluted with lumped disturbances. A new continuous terminal sliding mode-based active anti-disturbance control (CTSMBAADC) is proposed by innovatively introducing a finite-time disturbance observer (FTDO) in homogeneous continuous nonsingular terminal sliding mode control (HCNTSMC) law. The HCNTSMC scheme drives the states of the system to the reference setpoint in finite-time. Rigorous stability analysis of the feedback loop system is based on input-to-state stability (ISS) concept and more importantly Lyapunov theory. Real-time experiments are performed to validate the designed control law. Results witness that the proposed control structure offers superior performance in terms of robustness and accuracy while avoiding the singularity problem and significantly alleviating the chattering phenomenon.

Index Terms - Attitude control; Quadrotor aircraft; Nonsingular terminal sliding mode; Finite-time stability; Pixhawk autopilot.

I. INTRODUCTION

A. Context and Motivations

Unmanned Aerial Vehicles (UAV) can be broadly classified as fixed-wing [1] or multirotor type. Quadrotor is the most popular kind of multirotor aircraft owing to its particular flight mode, variety of sizes, and excellent hovering capabilities. Quadrotor has been extensively used in many fields [2] [3] [4] [5]. However, despite its catching features, a quadrotor suffers from crucial challenges particularly in terms of its control. Autonomous flight of a quadrotor is essentially dependent on accurate and robust attitude control of the aircraft. Substantially, since the quadrotor has an under-actuated nature, its position control is achieved by controlling the attitude subsystem [6] [7]. A quadrotor being an inherently nonlinear system with highly coupled dynamics involves internal modeling errors, parametric uncertainties and external disturbances. The controller design for the attitude system becomes an extremely challenging task. Therefore, the autonomous flight of this aircraft requires a sophisticated control scheme for meeting flight mission requirements. Moreover, robustness, high control precision, and fast convergence appear to be key factors in the controller design.

B. Literature Review

Modern control of the quadrotor aircrafts using robust control techniques including Sliding Mode Control (SMC) is an

active topic in UAV community [8]. Such a method offers design simplicity and fast response; besides, it can compensate theoretically exactly, bounded matched perturbations.

Several recently reported research works focused on using robust control laws based on SMC for disturbances handling in the quadrotor system. Research reported in [9] attempted to enhance stability of an underactuated quadcopter aircraft using integral SMC based scheme. Another interesting work [10] considered the quadrotor model with disturbances and proposed a robust backstepping SMC law. However, a linear switching manifold has been used and thus the states are ensured to converge only asymptotically to the origin. Moreover, Linear SMC (LSMC) exhibits chattering problem that can saturate the actuators and also suffers from low accuracy and depreciated performance issues. One way to overcome some of these problems is to have a nonlinear sliding manifold and employ Terminal SMC (TSMC) based control law that is aimed at achieving the convergence in finite-time [11]. Compared with LSMC, TSMC offers faster convergent response, however, it suffers from singularity and chattering. A variant, nonsingular TSMC (NTSMC) addresses the singularity problem. Going beyond NTSMC, research reported in [12] proposed an adaptive nonsingular fast TSMC with the objective to accurately track the reference trajectory. However, the response may be subjected to chattering phenomenon due to the discontinuous control signal involved. This phenomenon has been mitigated in this work by replacing $\text{sign}(\cdot)$ function with $\tanh(\cdot)$ function. In contrast, continuous SMC based control laws involving continuous signals are well known for their capability to eliminate chattering [2]. Continuous NTSMC (CNTSMC) offers improved precision and finite-time convergence. Considering a two links flexible arm, research in [13] proposed a CNTSMC based controller to realize robust control with uncertain conditions.

To the best of authors' knowledge, a small number of scientific contributions e.g. [2] and [14] investigate the continuous SMC based schemes for quadrotor aircrafts. A recently reported work [15] presents an adaptive SMC based disturbance observer for nonlinear system with uncertainties, However, the dynamics of the disturbance observer are not analyzed collectively with the stabilizing feedback controller. Inspired by [15], the primary focus of the present work is to present experimental results with an aim of bridging the gap between theoretical fronts and practical scenerios.

C. Contributions

The key scientific contributions of the present research can be summarized as:

- Robust design of a nonlinear controller to control the attitude of a quadrotor aircraft operating in an environment polluted with various disturbances. Owing to continuous nature of the designed control algorithm, chattering is avoided which is inherently present in works (e.g. [9], [10]) based on discontinuous SMC based schemes. Moreover, the present work avoids the singularity issue which is present in the traditional TSMC.
- In contrast to [15] the disturbance observer dynamics are analyzed jointly with the controller dynamics in the stability proof to ensure the boundedness of the error signals.
- Experimental comparative analysis using a real quadrotor platform is conducted.

This paper is organized in five sections. Section II presents preliminaries and states the problem focused in the paper. The control algorithm is proposed in Section III with a rigorous mathematical treatment on stability. Section IV presents the experimental results with a critical discussions on the obtained results. Finally, Section V concludes the paper and explores potential avenues for related research.

II. PRELIMINARIES AND PROBLEM STATEMENT

A. Preliminaries

Lemma 1. ([16]). (Global finite-time stability (GFTS)). If the parameters $b_i > 0$, $i = 1, \dots, n$ make the polynomial $p^n + b_n p^{n-1} + \dots + b_2 p + b_1$ be Hurwitz, i.e. all of its roots lie in the stable region (left half plane), the origin of the system given in (1)

$$\begin{cases} \dot{x}_i = x_{i+1}, & i = 1, \dots, n-1 \\ \dot{x}_n = -b_1 |x_1|^{\alpha_1} \text{sign}(x_1) - \dots - b_n |x_n|^{\alpha_n} \text{sign}(x_n). \end{cases} \quad (1)$$

is in stable equilibrium in finite-time in global context, where α_i are determined as: $\alpha_1 = \alpha$ for $n = 1$, and $\alpha_{i-1} = \frac{\alpha_i \alpha_{i+1}}{2\alpha_{i+1} - \alpha_i}$ for $i = 2, \dots, n \quad \forall n \geq 2$.

Lemma 2. ([15]). (Input-to-state stability (ISS)). Considering the system represented as $\dot{x} = F(x, v) = f(x) + g(x)v$ where $F: D \times D_v \rightarrow \mathbb{R}^n$ is locally Lipschitz in x , the domain $D \in \mathbb{R}^n$ involves $x = 0$, and the domain $D_v \in \mathbb{R}^m$ contains $v = 0$. If origin of system $\dot{x} = f(x)$ is stable asymptotically and $g(x)$ is continuously differentiable, then $\dot{x} = F(x, v)$ is locally ISS.

B. Problem Statement

The differential equations governing the acceleration dynamics corresponding to rotational motion of the quadrotor (Fig. 1) subjected to disturbances is represented as [2] [16],

$$\begin{cases} \ddot{\phi} = J_{xx}^{-1}[(J_{yy} - J_{zz})\dot{\theta}\dot{\psi} + u_\phi + d_\phi], \\ \ddot{\theta} = J_{yy}^{-1}[(J_{zz} - J_{xx})\dot{\phi}\dot{\psi} + u_\theta + d_\theta], \\ \ddot{\psi} = J_{zz}^{-1}[(J_{xx} - J_{yy})\dot{\phi}\dot{\theta} + u_\psi + d_\psi]. \end{cases} \quad (2)$$

where $\Phi, \theta, \psi \in \mathbb{R}$ are the Euler angles, $J_{xx}, J_{yy}, J_{zz} \in \mathbb{R}_+$ represent the moments of inertia, $u_\phi, u_\theta, u_\psi \in \mathbb{R}$ are the control inputs and $d_\phi, d_\theta, d_\psi \in \mathbb{R}$ denote the lumped disturbances including parametric uncertainties, unmodeled dynamics and external disturbances.

For the sake of generalization, the model given in (2) can consider the attitude dynamics as a 2nd order perturbed nonlinear system. Hence, the model used in the design of control law can be written as

$$\begin{cases} \dot{x}_1(t) = x_2(t), \\ \dot{x}_2(t) = f_\eta(x, t) + g_\eta(x, t)u_\eta(t) + d_\eta(x, t). \end{cases} \quad (3)$$

here $x \stackrel{\text{def}}{=} [x_1, x_2]^T \in \mathbb{R}^2$ is the state vector, where $x_1 \stackrel{\text{def}}{=} \eta = [\Phi, \theta, \psi]^T \in \mathbb{R}^3$, $x_2 \stackrel{\text{def}}{=} \dot{\eta} = [\dot{\Phi}, \dot{\theta}, \dot{\psi}]^T \in \mathbb{R}^3$, and $d_\eta(x, t) \stackrel{\text{def}}{=} [d_\phi, d_\theta, d_\psi]^T \in \mathbb{R}^3$ is the overall lumped disturbance satisfying $\|d_\eta\| \leq L_{d_\eta}$ for a bounded Lipschitz constant $L_{d_\eta} < \infty$, $u_\eta \stackrel{\text{def}}{=} [u_\phi, u_\theta, u_\psi]^T$ is the control input vector. $f_\eta(x, t), g_\eta(x, t) \neq 0$ are nonlinear differentiable functions defined as

$$\begin{cases} f_\phi(x, t) \stackrel{\text{def}}{=} J_{xx}^{-1}(J_{yy} - J_{zz})\dot{\theta}\dot{\psi}, & g_\phi \stackrel{\text{def}}{=} J_{xx}^{-1}, \\ f_\theta(x, t) \stackrel{\text{def}}{=} J_{yy}^{-1}(J_{zz} - J_{xx})\dot{\phi}\dot{\psi}, & g_\theta \stackrel{\text{def}}{=} J_{yy}^{-1}, \\ f_\psi(x, t) \stackrel{\text{def}}{=} J_{zz}^{-1}(J_{xx} - J_{yy})\dot{\phi}\dot{\theta}, & g_\psi \stackrel{\text{def}}{=} J_{zz}^{-1}. \end{cases} \quad (4)$$

Remark 1. The unmodeled dynamics in the present work include aerodynamical and gyroscopic effect moments. These are not taken into account in the design of the control law. Therefore, they will be considered as disturbances.

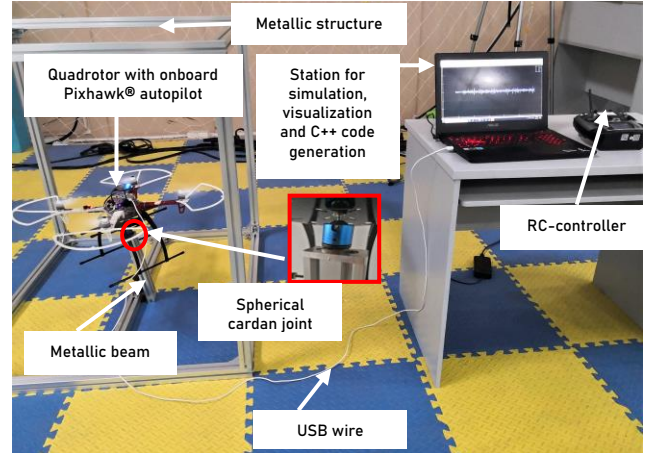


Fig. 1. Experiment setup for the quadrotor's attitude control.

Definition 1. The considered control problem comprises of design of a finite-time robust control law $u_\eta = [u_\phi, u_\theta, u_\psi]^T$ for the attitude system subjected to perturbations in (3), such that

- Errors in tracking the attitude reference approach to the origin in a finite-time T_c , i.e., $\eta(t) - \eta_d(t) \equiv 0, \forall t \geq T_c$.
- The designed control law should demonstrate good robust response against lumped disturbances and non-linearities.
- The control signal is continuous, nonsingular and is free from chattering issues.

III. CONTROL DESIGN AND STABILITY ANALYSIS

A. Finite-Time Disturbance Observer (FTDO) Design

Considering the model given in (3) under the influence of external disturbances, design of a FTDO can be given as

$$\begin{cases} \dot{\gamma}_0 = \Lambda_0 + f_\eta + g_\eta u_\eta, \\ \Lambda_0 = -\rho_1 L_{d_\eta}^{1/3} \text{sign}^{2/3}(\gamma_0 - \dot{\eta}) + \gamma_1, \\ \dot{\gamma}_1 = \Lambda_1, \\ \Lambda_1 = -\rho_2 L_{d_\eta}^{1/2} \text{sign}^{1/2}(\gamma_1 - \Lambda_0) + \gamma_2, \\ \dot{\gamma}_2 = -\rho_3 L_{d_\eta} \text{sign}(\gamma_2 - \Lambda_1). \end{cases} \quad (5)$$

in which ρ_1, ρ_2, ρ_3 and L_{d_η} are constants, where $L_{d_\eta} > 0$ and $\rho_1, \rho_2, \rho_3 > 0$. Besides, γ_0, γ_1 and γ_2 are estimates of $\dot{\eta}, d_\eta$ and \hat{d}_η , respectively.

B. Homogeneous Continuous Nonsingular Terminal Sliding Mode Control Design

Defining the attitude tracking error and its dynamics as

$$\begin{cases} e_\eta \stackrel{\text{def}}{=} \eta - \eta_d, \\ \varrho_\eta \stackrel{\text{def}}{=} \dot{\eta} - \dot{\eta}_d. \end{cases} \quad (6)$$

The derivative of (6) w.r.t. yields to

$$\begin{cases} \dot{e}_\eta = \varrho_\eta, \\ \dot{\varrho}_\eta = \ddot{\eta} - \ddot{\eta}_d. \end{cases} \quad (7)$$

HCNTSMC manifold for ensuring accurate performance of the attitude control system is defined as,

$$s_\eta \stackrel{\text{def}}{=} \dot{\varrho}_\eta + k_{\eta_1} |e_\eta|^{\alpha_1} \text{sign}(e_\eta) + k_{\eta_2} |\varrho_\eta|^{\alpha_2} \text{sign}(\varrho_\eta). \quad (8)$$

where $k_{\eta_1} := [k_{\phi_1}, k_{\theta_1}, k_{\psi_1}]^T, k_{\eta_2} := [k_{\phi_2}, k_{\theta_2}, k_{\psi_2}]^T \in \mathbb{R}_+^3$ and $\alpha_1, \alpha_2 \in \mathbb{R}_+$ are some constants. The control input required to demonstrate the reaching phase of the manifold s_η and sliding motion on $s_\eta = 0$ is designed as,

$$u_\eta \stackrel{\text{def}}{=} u_{e_{q_\eta}} + g_\eta^{-1} u_{n_\eta}. \quad (9)$$

The sliding motion $s_\eta = 0$ is used to obtain $u_{e_{q_\eta}}$ (equivalent control term). The dynamics of the sliding manifold when the feedback-loop system is approaching to the sliding surface $s_\eta = 0$ can be written as

$$\dot{\eta} - \dot{\eta}_d + k_{\eta_1} |e_\eta|^{\alpha_1} \text{sign}(e_\eta) + k_{\eta_2} |\varrho_\eta|^{\alpha_2} \text{sign}(\varrho_\eta) = 0, \quad (10)$$

Substituting $\dot{\eta}$ by its expression from (3) into (10), and after some manipulations, $u_{e_{q_\eta}}$ can be obtained

$$u_{e_{q_\eta}} \stackrel{\text{def}}{=} g_\eta^{-1} (-f_\eta - k_{\eta_1} |e_\eta|^{\alpha_1} \text{sign}(e_\eta) - k_{\eta_2} |\varrho_\eta|^{\alpha_2} \text{sign}(\varrho_\eta) - \hat{d}_\eta + \dot{\eta}_d). \quad (11)$$

The reaching control term u_{n_η} ensures reaching of the sliding manifold in finite-time and is proposed as

$$\begin{cases} \dot{u}_{n_\eta} + \mu_\eta u_{n_\eta} = u_{s_\eta}, & u_{n_\eta}(0) = 0 \\ u_{s_\eta} = -\left(v_\eta + \mu_\eta |u_{n_\eta}|\right) \text{sign}(s_\eta). \end{cases} \quad (12)$$

where $\mu_\eta, v_\eta \in \mathbb{R}_+$ are positive constants.

C. Stability Analysis for the Feedback-Loop System

Theorem 1. For the nonlinear rotational system (3) with total disturbances d_η , under the terminal sliding mode surface s_η given by (8), and the HCNTSMC control law u_η (9) together with the FTDO dynamics (5) can guarantee that all signals in the feedback-loop system are bounded and ensure that the tracking errors are GFTS.

Proof. The proof is given in three consecutive steps.

Step 1. We prove here that the sliding surface s_η demonstrate finite-time convergence to the equilibrium. Putting $\dot{\eta}$ from (3) into the sliding manifold s_η in (8), we get

$$s_\eta = f_\eta + g_\eta u_\eta + d_\eta - \dot{\eta}_d + k_{\eta_1} |e_\eta|^{\alpha_1} \text{sign}(e_\eta) + k_{\eta_2} |\varrho_\eta|^{\alpha_2} \text{sign}(\varrho_\eta), \quad (13)$$

By putting the control law u_η (9) into s_η (13), the dynamics of the sliding manifold can be written as

$$s_\eta = u_{n_\eta} + d_\eta - \hat{d}_\eta, \quad (14)$$

Furthermore, according to the preceding analysis, the disturbances d_η can be estimated by the FTDO observer, hence $d_\eta \equiv \hat{d}_\eta$, and thereby

$$s_\eta = u_{n_\eta}, \quad (15)$$

By differentiating (15) and substituting (12), one achieves

$$\dot{s}_\eta = \dot{u}_{n_\eta} = -\left(v_\eta + \mu_\eta |u_{n_\eta}|\right) \text{sign}(s_\eta) - \mu_\eta u_{n_\eta}. \quad (16)$$

Selecting the positive-definite Lyapunov function as

$$V_\eta \stackrel{\text{def}}{=} s_\eta^2 / 2, \quad (17)$$

By differentiating V_η and then substituting (16), we get

$$\begin{aligned} \dot{V}_\eta &= s_\eta \dot{s}_\eta = s_\eta \left[-\left(v_\eta + \mu_\eta |u_{n_\eta}|\right) \text{sign}(s_\eta) - \mu_\eta u_{n_\eta} \right], \\ &\leq -v_\eta |s_\eta| \leq 0. \end{aligned} \quad (18)$$

Then, it has $v_\eta > 0$. Hence, this proves that the sliding manifold converges to zero $s_\eta = 0$ in finite-time.

Step 2. We show that the dynamics of the sliding mode variable s_η and disturbance estimation error $e_{ob_2} \stackrel{\text{def}}{=} \gamma_1 - d_\eta$ will not drive the error variables (e_η, \dot{e}_η) to infinity. Recalling the errors dynamics from (6). Let us define $\bar{x}_1 \stackrel{\text{def}}{=} e_\eta, \bar{x}_2 \stackrel{\text{def}}{=} \dot{e}_\eta = \varrho_\eta$ and $\bar{x} \stackrel{\text{def}}{=} [\bar{x}_1, \bar{x}_2]^T$. Then, the dynamics of the feedback-loop system (6) are rewritten as

$$\begin{cases} \dot{\bar{x}}_1 = \bar{x}_2, \\ \dot{\bar{x}}_2 = f_\eta + g_\eta u_\eta + d_\eta - \dot{\eta}_d, \end{cases} \quad (19)$$

Considering s_η designed in (8), the dynamics of the perturbed system given in (19) are written as

$$\begin{cases} \dot{\bar{x}}_1 = \bar{x}_2, \\ \dot{\bar{x}}_2 = -k_{\eta_1} |\bar{x}_1|^{\alpha_1} \text{sign}(\bar{x}_1) - k_{\eta_2} |\bar{x}_2|^{\alpha_2} \text{sign}(\bar{x}_2) + s_\eta - e_{ob_2}. \end{cases} \quad (20)$$

From (20), we can see that the sliding surface s_η and the observation error e_{ob_2} are included in the $\dot{\bar{x}}_2$ dynamics. Now, let us define the following finite-time bounded function for the closed loop-system (20) including sliding surface dynamics and tracking error dynamics

$$V(s_\eta, \bar{x}_1, \bar{x}_2) \stackrel{\text{def}}{=} (s_\eta^2 + \bar{x}_1^2 + \bar{x}_2^2)/2, \quad (21)$$

Note that $|\bar{x}_1|^{\alpha_1} \leq 1 + |\bar{x}_1|$ and $|\bar{x}_2|^{\alpha_2} \leq 1 + |\bar{x}_2|$ for $0 < \alpha_1, \alpha_2 < 1$. Differentiating V along the system (20), one gets $\dot{V} = s_\eta \dot{s}_\eta + \bar{x}_1 \dot{\bar{x}}_1 + \bar{x}_2 \dot{\bar{x}}_2$,

$$\begin{aligned} &= s_\eta \left[-\left(v_\eta + \mu_\eta |u_{n_\eta}| \right) \text{sign}(s_\eta) - \mu_\eta u_{n_\eta} \right] + \bar{x}_1 \bar{x}_2 + \\ &\bar{x}_2 \left[-k_{\eta_1} |\bar{x}_1|^{\alpha_1} \text{sign}(\bar{x}_1) - k_{\eta_2} |\bar{x}_2|^{\alpha_2} \text{sign}(\bar{x}_2) + s_\eta - e_{ob_2} \right], \\ &\leq -v_\eta |s_\eta| - \mu_\eta |s_\eta| |u_{n_\eta}| + \mu_\eta |s_\eta| |u_{n_\eta}| + \bar{x}_1 \bar{x}_2 + \\ &\bar{x}_2 \left[-k_{\eta_1} (1 + |\bar{x}_1|) - k_{\eta_2} (1 + |\bar{x}_2|) + s_\eta - e_{ob_2} \right], \\ &\leq -v_\eta |s_\eta| + |\bar{x}_1 \bar{x}_2| + k_{\eta_1} |\bar{x}_1 \bar{x}_2| + (k_{\eta_1} + k_{\eta_2}) |\bar{x}_2| + \\ &k_{\eta_2} |\bar{x}_2 \bar{x}_2| + |\bar{x}_2 s_\eta| + |\bar{x}_2 e_{ob_2}|, \\ &\leq -v_\eta \frac{1+s_\eta^2}{2} + \frac{\bar{x}_1^2 + \bar{x}_2^2}{2} + k_{\eta_1} \frac{\bar{x}_1^2 + \bar{x}_2^2}{2} + (k_{\eta_1} + k_{\eta_2}) \frac{1 + \bar{x}_2^2}{2} + \\ &k_{\eta_2} \frac{\bar{x}_2^2 + \bar{x}_2^2}{2} + \frac{\bar{x}_2^2 + s_\eta^2}{2} + \frac{\bar{x}_2^2 + e_{ob_2}^2}{2}, \\ &\leq K_V V + L_V. \end{aligned} \quad (22)$$

where $K_V \stackrel{\text{def}}{=} \max\{1 - v_\eta, 1 + k_{\eta_1}, 2k_{\eta_1} + 3k_{\eta_2} + 3\}$, and $L_V \stackrel{\text{def}}{=} \max\{-v_\eta + k_{\eta_1} + k_{\eta_2} + \frac{e_{ob_2}^2}{2}\}$ are bounded constants. Thus, it can be concluded from (22) that $V(s_\eta, \bar{x}_1, \bar{x}_2)$ and so $s_\eta, \bar{x}_1 = e_\eta, \bar{x}_2 = \hat{e}_\eta$ will not lead to ∞ in finite-time.

Step 3. This step shows the finite-time convergence of tracking error e_η to the origin along with the surface $s_\eta = 0$ after reaching the sliding manifold. With $s_\eta = 0$, using (10) and taking $\bar{x}_1 = e_\eta, \bar{x}_2 = \hat{e}_\eta$, one has

$$\dot{\eta} = \dot{\eta}_d - k_{\eta_1} |\bar{x}_1|^{\alpha_1} \text{sign}(\bar{x}_1) - k_{\eta_2} |\bar{x}_2|^{\alpha_2} \text{sign}(\bar{x}_2) \quad (23)$$

Recalling the errors dynamics from (6) with $\bar{x} = [\bar{x}_1, \bar{x}_2]^T$

$$\begin{cases} \dot{\bar{x}}_1 = \bar{x}_2, \\ \dot{\bar{x}}_2 = \dot{\eta} - \dot{\eta}_d, \end{cases} \quad (24)$$

Substituting (23) into error dynamics' expressions, one gets

$$\begin{cases} \dot{\bar{x}}_1 = \bar{x}_2, \\ \dot{\bar{x}}_2 = -k_{\eta_1} |\bar{x}_1|^{\alpha_1} \text{sign}(\bar{x}_1) - k_{\eta_2} |\bar{x}_2|^{\alpha_2} \text{sign}(\bar{x}_2). \end{cases} \quad (25)$$

The stabilization of the tracking error (e_η, \hat{e}_η) to zero along $s_\eta = 0$ follows from Lemma 1. Thus, they are guaranteed to be GFTS. Hence, this proves the finite-time stability of the attitude control system.

Theorem 2. The perturbed system given in (3) can be controlled by applying the designed law u_η (9), which guarantees ISS of the feedback-loop attitude system inspite of the presence of disturbances.

Proof. The dynamics of the feedback-loop system after application of the control input (9) to the system (3) can be written as

$$\begin{cases} \dot{\chi}_1(t) = \chi_2(t), \\ \dot{\chi}_2(t) = F_\eta(X, u_{n_\eta}, t). \end{cases} \quad (26)$$

where F_η is defined as

$$F_\eta \stackrel{\text{def}}{=} -k_{\eta_1} |\bar{x}_1|^{\alpha_1} \text{sign}(\bar{x}_1) - k_{\eta_2} |\bar{x}_2|^{\alpha_2} \text{sign}(\bar{x}_2) + u_{n_\eta} + d_\eta - \hat{d}_\eta + \dot{\eta}_d. \quad (27)$$

Using the errors dynamics from (24) and then substituting (3), the following feedback-loop system with disturbances input is obtained

$$\begin{cases} \dot{\bar{x}}_1 = \bar{x}_2, \\ \dot{\bar{x}}_2 = -k_{\eta_1} |\bar{x}_1|^{\alpha_1} \text{sign}(\bar{x}_1) - k_{\eta_2} |\bar{x}_2|^{\alpha_2} \text{sign}(\bar{x}_2) + \bar{u}_\eta, \end{cases} \quad (28)$$

The above system (28) can be formulated as

$$\dot{\bar{x}} \stackrel{\text{def}}{=} a_\eta(\bar{x}) + \mathcal{B}_\eta \bar{u}_\eta, \quad (29)$$

where $a_\eta(\bar{x})$, \mathcal{B}_η and the input \bar{u}_η are defined as

$$a_\eta(\bar{x}) \stackrel{\text{def}}{=} \begin{bmatrix} \bar{x}_2 \\ -k_{\eta_1} |\bar{x}_1|^{\alpha_1} \text{sign}(\bar{x}_1) - k_{\eta_2} |\bar{x}_2|^{\alpha_2} \text{sign}(\bar{x}_2) \end{bmatrix}, \quad (30)$$

$$\mathcal{B}_\eta \stackrel{\text{def}}{=} [0 \quad 1]^T, \bar{u}_\eta \stackrel{\text{def}}{=} u_{n_\eta} + d_\eta - \hat{d}_\eta. \quad (31)$$

where u_{n_η} is the control input. The disturbances input and its estimate are denoted by d_η and \hat{d}_η respectively. Since the observation error e_{ob_2} is bounded, it can be shown that u_{n_η} is bounded as in [15]: $|u_{n_\eta} + d_\eta - \hat{d}_\eta| \leq |u_{n_\eta}| + |d_\eta - \hat{d}_\eta| \leq 2|e_{ob_2}|$. It follows from Lemma 1 that the autonomous system $\dot{\bar{x}} = a_\eta(\bar{x})$ demonstrates finite-time stability and hence the system is asymptotically stable. Furthermore, the system $\dot{\bar{x}} = a_\eta(\bar{x}) + \mathcal{B}_\eta \bar{u}_\eta$ given by (30) satisfies the conditions of Lemma 2, thus it is locally ISS w.r.t the input signal despite the disturbances. Thereby, the angular signals remain bounded while the bounded input signal \bar{u}_η is applied to the attitude system, which completes the proof.

IV. EXPERIMENT RESULTS AND DISCUSSIONS

A. Software and Hardware Configuration

The theoretical design has been validated by conducting experiments on a quadrotor aircraft platform illustrated in Fig. 1. The proposed control law is realized on an onboard flight controller Pixhawk[®]. Considering the physical parameters of the aircraft as: $m = 1.636$ kg, $l = 0.225$ m, $J_{xx} = 0.0232$ kg m², $J_{yy} = 0.0249$ kg m², $J_{zz} = 0.0342$ kg m². Table I lists the control parameters.

TABLE I
PARAMETERS OF CONTROLLER AND OBSERVER.

Parameter	Value	Parameter	Value
k_{ϕ_1}	40	v_η	0.001
$k_{\theta_1} = k_{\psi_1}$	30	μ_η	0.1
k_{ϕ_2}	23	ρ_1	2
$k_{\theta_2} = k_{\psi_2}$	16.5	ρ_2	4.5
α_1	0.5385	ρ_3	2
α_2	0.70	L_{d_η}	1.2

B. Stabilization Experiment

The purpose of this experiment is to demonstrate that the designed control algorithm can stabilize the attitude to the origin, i.e., $\eta_d = [0, 0, 0]^T$ deg, from a random given initial position of $\eta_0 = [\Phi_0, \theta_0, \psi_0]^T = [20, -20, 15]^T$ deg. This situation resembles a flight hoversy in reality. The attitude response is illustrated in Fig. 2. It is observed that the proposed

control law can drive the attitude states (Φ, θ, ψ) from initial angles that are far from zero to the origin in finite-time for all the variables.

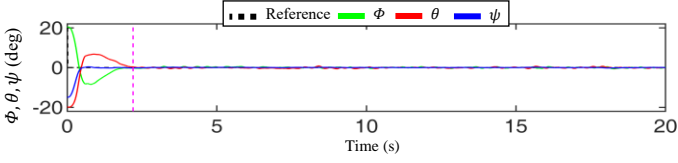


Fig. 2. Convergence of the states (Φ, θ, ψ) to the origin.

C. Tracking Experiment

The attitude reference trajectory is given as

$$[\Phi_d, \theta_d, \psi_d]^T \stackrel{\text{def}}{=} [-10\sin(0.1\pi t), 10\sin(0.1\pi t), 15\cos(0.1\pi t)]^T.$$

Fig. 3 shows the actual and reference tracking states while Fig. 4 presents the corresponding tracking errors. As illustrated, the proposed CTSMBAADC law permits accurate and robust tracking of the reference trajectory.

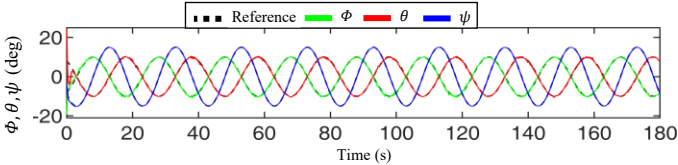


Fig. 3. Orientation (Φ, θ, ψ) for the tracking task.

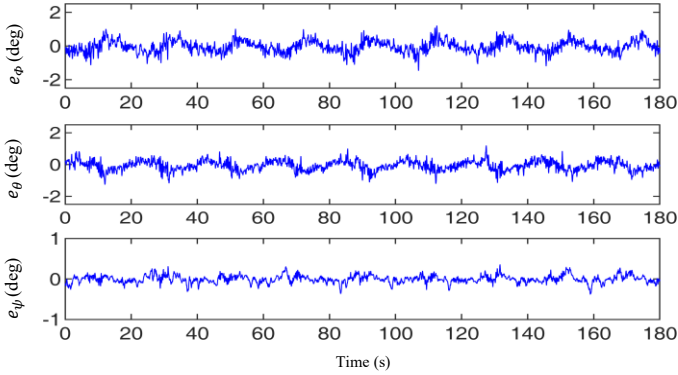


Fig. 4. Tracking error signals $(e_\phi, e_\theta, e_\psi)$.

D. Robustness and Disturbance Rejection Experiments

To quantify the superior performance achieved by the presented control law, series of experiments comparing various robust controllers are conducted. The controllers include; CTSMBAADC, backstepping sliding mode controller (BSSMC) [10], twisting controller (TC) [14], and ANFTSMC [12]. A load of 117gm is attached to the edge of the arm of the quadrotor. Comparative results are provided in Fig. 5 where robust response offered by all the control techniques is evident. The techniques converge the orientation variables to the reference with the application of sustained load disturbance and abrupt variations in the reference setpoints. The preliminary analysis of orientation's signals can show the high coupling of the attitude dynamics notably in the presence of disturbances. Since each degree of freedom is affected by the change of the other states. Hence, the peaks can be seen in the plots at the time one variable tracks a given set-point. The orientation errors are

depicted in Fig. 6. This figure confirms that the null steady-state error is achieved for the attitude states.

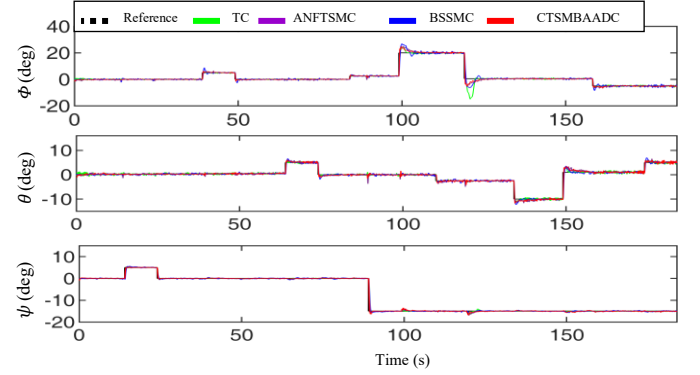


Fig. 5. Orientation (Φ, θ, ψ) : Comparison under load disturbance.

Various standard performance indexes are used to characterize the comparison of the results achieved. These include Integral of the Absolute value of the Derivative of the input u (IADU) and Integral of Square Error (ISE). These criteria are defined as $ISE \stackrel{\text{def}}{=} \int_{t_i}^{t_f} e_\eta(\tau)^2 d\tau$, $IADU \stackrel{\text{def}}{=} \int_{t_i}^{t_f} \left| \frac{du_\eta(\tau)}{d\tau} \right| d\tau$. TABLE II presents the calculated values corresponding to these indexes.

TABLE II
ISE AND IADU PERFORMANCE INDEXES FOR ATTITUDE CONTROL.

Control strategy	Performance index					
	ISE		IADU			
	ϕ	θ	ψ	ϕ	θ	ψ
TC	0.089	0.076	0.04527	3.290	3.394	3.116
BSSMC	0.109	0.092	0.04537	7.921	3.183	1.209
ANFTSMC	0.097	0.068	0.02768	3.028	2.694	1.182
CTSMBAADC	0.066	0.064	0.02512	1.425	1.610	0.535

It is clear from the Table that CTSMBAADC improves the accuracy in all the states. It can also be observed that ANFTSMC and TC controllers offer acceptable performance. Moreover, CTSMBAADC based law offers smoother response compared to the other controllers under discussion. Meanwhile, TC [14] and ANFTSMC [12] also allow mitigation of the chattering effect shown by BSSMC [10] approach by providing smoother control signals. Finally, the identified disturbances and control signals are shown in Fig. 7 and Fig. 8 respectively.

V. CONCLUSION

Considering a quadrotor system, this research proposed a CTSMBAADC approach to design an accurate and robust attitude control law. A control strategy has been designed while considering model uncertainties and disturbances externally acting on the rotational system. The control structure has been developed by combining an FTDO observer for unknown disturbances canceling and a HCNTSMC scheme to ensure finite-time convergence and singularity-free continuous control. Also, the stability of the feedback-loop system has been rigorously discussed and proved. Results based on the experimental trials on a quadrotor aircraft are found to be consistent with the theoretical foundations. To thoroughly investigate the capabilities of the designed control law, a

comparative analysis based on various performance indexes is carried out. Results witness the effectiveness and superiority of the proposed control law in terms of robustness, accuracy and elimination of chattering phenomenon. Further studies will concentrate on the cartesian trajectory tracking with a real outdoor flight experiment.

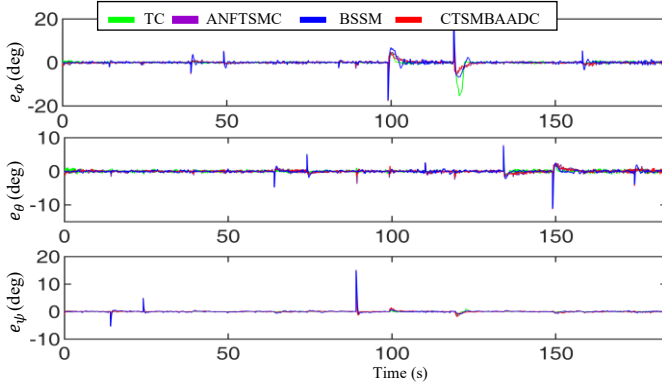


Fig. 6. Orientation errors (e_ϕ, e_θ, e_ψ): Comparison under load disturbance.

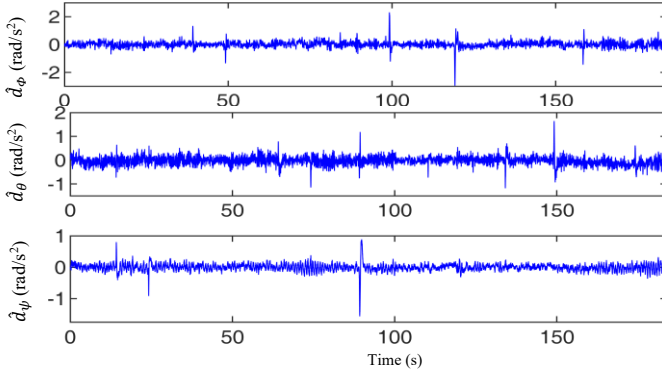


Fig. 7. Disturbance identification ($\hat{d}_\phi, \hat{d}_\theta, \hat{d}_\psi$): Sustained load disturbance.

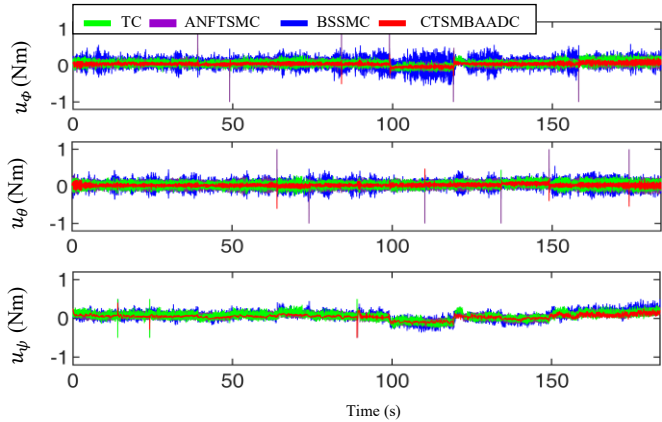


Fig. 8. Control signals (u_ϕ, u_θ, u_ψ): Comparison under load disturbance.

ACKNOWLEDGMENT

This work was supported by the National Natural Science Foundation of China under Grant No. 61803075, the Fundamental Research Funds for the Central Universities under Grants No. ZYGX2018KYQD211 and No. ZYGX2019J084.

- [1] M. Wasim, M. Ullah and J. Iqbal, "Gain-scheduled proportional integral derivative control of taxi model of unmanned aerial vehicles," *Revue Roumaine des Sciences Techniques-Serie Electrotechniqueet Energetique*, vol. 64, no. 1, pp. 75-80, 2019.
- [2] O. Mechali, L. Xu, Y. Huang, M. Shi and X. Xie, "Observer-based fixed-time continuous nonsingular terminal sliding mode control of quadrotor aircraft under uncertainties and disturbances for robust trajectory tracking: Theory and experiment," *Control Engineering Practice*, vol. 111, pp. 1-23, 2021.
- [3] O. Mechali, L. Xu, A. Senouci, X. Xie, C. Xin and A. Mechali, "Finite-time observer-based robust continuous twisting control for the attitude of an uncertain quadrotor UAV subjected to disturbances," in *IEEE ICMA*, Beijing, China, 2020.
- [4] O. Mechali, L. Xu, M. Wei, F. Guo and A. Senouci, "A rectified RRT* with efficient obstacles avoidance method for UAV in 3D environment," in *2019 IEEE CYBER*, Suzhou, China, 2020.
- [5] O. Mechali, J. Iqbal, J. Wang, X. Xie and L. Xu, "Distributed leader-follower formation control of quadrotors swarm subjected to disturbances," in *IEEE ICMA*, Takamatsu, Japan, 2021.
- [6] S. Ullah, Q. Khan, A. Mehmood, S. A. M. Kirman and O. Mechali, "Neuro-adaptive fast integral terminal sliding mode control design with variable gain robust exact differentiator for under-actuated quadcopter UAV," *ISA Transactions*, 2021.
- [7] G. Fan, W. Mingzhu, Y. Mingfei, L. Jiajun, O. Mechali and Y. Cao, "An unmanned aerial vehicles collaborative searching and tracking scheme in three-dimension space," in *2019 IEEE CYBER*, Suzhou, China, 2020.
- [8] S. G. Khan, S. Bendoukha, W. Naeem and J. Iqbal, "Experimental validation of an integral sliding mode-based LQG for the pitch control of a UAV-mimicking platform," *Advances in Electrical and Electronics Engineering*, vol. 17, no. 3, pp. 275-284, 2019.
- [9] S. Ullah, A. Mehmood, Q. Khan, S. Rehman and J. Iqbal, "Robust integral sliding mode control design for stability enhancement of under-actuated quadcopter," *International Journal of Control, Automation and Systems*, vol. 18, no. 7, pp. 1671-1678, 2020.
- [10] D. J. Almahles, "Robust Backstepping Sliding Mode Control for a Quadrotor Trajectory Tracking Application," *IEEE Access*, vol. 8, pp. 5515-5525, 2020.
- [11] M. Zhihong and X. H. Yu, "Terminal sliding mode control of MIMO linear systems," *IEEE Transactions on Circuits and Systems I: Fundamental Theory and Applications*, vol. 44, no. 11, pp. 1065-1070, 1997.
- [12] M. Labbadi and M. Cherkaoui, "Robust adaptive nonsingular fast terminal sliding mode tracking control for an uncertain quadrotor UAV subjected to disturbances," *ISA Transactions*, vol. 99, pp. 290-304, 2020.
- [13] Y. Wang, F. Han, Y. Feng and H. Xia, "Hybrid continuous nonsingular terminal sliding mode control of uncertain flexible manipulators," in *IECON 2014 - 40th Annual Conference of the IEEE Industrial Electronics Society*, Dallas, TX, USA, 2015.
- [14] R. Falc3n, H. R3os and A. Dzul, "Comparative analysis of continuous sliding-modes control strategies for quad-rotor robust tracking," *Control Engineering Practice*, vol. 90, pp. 241-256, 2019.
- [15] H. Rabiee, M. Ataei and M. Ekramian, "Continuous nonsingular terminal sliding mode control based on adaptive sliding mode disturbance observer for uncertain nonlinear systems," *Automatica*, vol. 109, pp. 1-7, 2019.
- [16] O. Mechali, J. Iqbal, X. Xie, L. Xu and A. Senouci, "Robust finite-time trajectory tracking control of quadrotor aircraft via terminal sliding mode-based active antidisturbance approach: A PIL experiment," *International Journal of Aerospace Engineering*, Vols. 2021, Article ID 5522379, pp. 1-28, 2021.